JOURNAL OF CATALYSIS 123, 74–85 (1990)

Gas-Phase Hydrodenitrogenation Reactions of Polynuclear Heteroaromatic Nitrogen Compounds and Selected Intermediates with a 50% Nickel Oxide/Aluminate Supported on Silica–Alumina Catalyst[1]

RICHARD H. FISH,*,[2] JAMES N. MICHAELS,† RILEY S. MOORE,*,† AND HEINZ HEINEMANN*

*Lawrence Berkeley Laboratory and †Department of Chemical Engineering, University of California, Berkeley, California 94720

Received September 25, 1989; revised November 22, 1989

The gas-phase hydrodenitrogenation (HDN) of quinoline 1,2,3,4-tetrahydroquinoline, 2-propylaniline, and propylbenzene with a 50% nickel oxide/aluminate on SiO_2–Al_2O_3 catalyst has been studied at 250°C under 1 atm of hydrogen gas. Under these mild conditions, alkylaromatics are the predominant HDN products. In the reaction network of this catalytic process, quinoline is hydrogenated to 1,2,3,4-tetrahydroquinoline, which subsequently undergoes C–N bond hydrogenolysis to form 2-propylaniline and then propylbenzene. Significant alkyl side-chain hydrogenolysis occurs in parallel to these reactions, producing a mixture of alkylanilines and alkylbenzenes. Small amounts of alkylcyclohexanes are produced by hydrogenation of the alkylbenzenes. This network differs significantly from that of commercial HDN processes in which quinoline is hydrogenated fully to decahydroquinoline prior to C–H bond cleavage. Pseudo-first-order rate constants have been estimated for quinoline hydrogenation, alkylaniline formation, alkylaniline HDN, and alkylbenzene hydrogenation and compared to analogous data for commercial HDN. This comparison indicates that the activity of the nickel oxide/aluminate on SiO_2–Al_2O_3 catalyst is within an order of magnitude of the activity of commercial HDN catalysts. The nickel oxide catalyst is irreversibly poisoned by sulfur and slowly deactivates during HDN due to coke formation; the coked catalyst can be regenerated by oxidation in air and subsequent reduction in hydrogen.

I. INTRODUCTION

The hydrodenitrogenation process (HDN) removes the nitrogen atom from polynuclear heteroaromatic nitrogen compounds as ammonia. The process is conducted over a variety of heterogeneous catalysts under strongly reducing conditions; 350–500°C and 150 bar are not unusual (*1–9*). These extreme conditions favor the complete reduction of both heteroaromatic and aromatic rings prior to nitrogen removal, and this accounts for the excessive use of hydrogen in HDN. For this reason, there is great interest in developing alternate catalysts that promote HDN under milder conditions.

Unfortunately, selective HDN is thermodynamically unfavorable, since carbon–nitrogen multiple bond cleavage is less favorable than carbon–carbon multiple bond cleavage. However, the converse is true for single carbon–nitrogen bonds: hydrogenolysis of alkylcarbon–nitrogen bonds is 5 kcal/mol more exothermic than that of aliphatic carbon–carbon bonds. For this reason, a selective HDN catalyst is one that promotes regioselective hydrogenation of the nitrogen-containing heteroaromatic ring followed by facile carbon–nitrogen bond hydrogenolysis.

Previous studies in our laboratory with

[1] The submitted manuscript has been authored by a contractor of the U.S. government under contract DE-AC03-76SF00098. Accordingly, the U.S. government retains a nonexclusive, royalty-free license to publish or reproduce the published form of this contribution, or allow others to do so, for U.S. government purposes.

[2] To whom all correspondence should be addressed.

0021-9517/90 $3.00

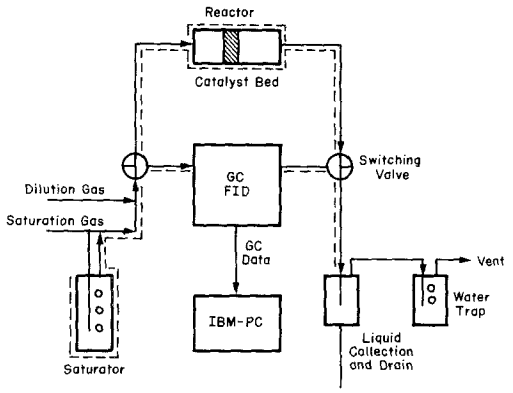

FIG. 1. Schematic of experimental apparatus.

homogeneous and polymer-supported transition metal catalysts demonstrated regioselective reduction of polynuclear heteroaromatic nitrogen compounds at low temperatures and hydrogen partial pressures (*10–15*). Unfortunately, these catalysts were inactive for cleaving alkylcarbon–nitrogen bonds. However, recently, we reported on a highly loaded nickel oxide/aluminate on silica–alumina catalyst that promoted the HDN reaction of 1,2,3,4-tetrahydroquinoline to anilines, alkylbenzenes, methane, and ammonia at 250°C and 1 atm of hydrogen (*16*). In this paper, we present a more complete kinetic study of gas-phase hydrodenitrogenation of quinoline, 1,2,3,4-tetrahydroquinoline, and selected intermediates with this catalyst under mild conditions. We propose a reaction network for this system and compare it to that of commercial HDN catalysts operating at higher temperatures and higher hydrogen pressures. Finally, we report on poisoning studies with H_2S and ammonia, as well as XPS and TEM studies of new, used, and sulfided samples of the catalyst.

II. EXPERIMENTAL

1. Materials

Quinoline (96%, Aldrich), 1,2,3,4-tetrahydroquinoline (98%, Aldrich), and 5,6,7,8-tetrahydroqinoline (96%, Aldrich), 2-propylaniline (97%, Lancaster Synthesis), and propylbenzene (97%, Alfa) were used as delivered. GC analysis indicated that these substrates met or exceeded purity specifications. Hydrogen (99.99%, Linde) and anhydrous ammonia (99.99%, Matheson) were filtered through a 2-μm filter prior to use.

The Ni/SiO_2–Al_2O_3 catalyst (50% Ni, 26% SiO_2, United Catalyst C46-7-03) was delivered as $\frac{1}{16} \times \frac{1}{8}$-in. pellets and used without modifications. The catalyst had a reported surface area of 250–350 m^2/g and a nickel dispersion of 22%. As is discussed below, the supported nickel was not fully reduced, but rather existed on the support as an oxide and/or an aluminate; for simplicity, we refer to it as 50% Ni/SiO_2–Al_2O_3.

2. Instrumentation

Reactions were carried out isobarically and isothermally in a continuous flow tubular reactor fabricated from 5- to 12-cm lengths of 0.64-cm-diameter Type 316 stainless-steel tubing. A fresh charge of 0.25 to 1.80 g of catalyst was used in each experimental run; the catalyst was held in place in the reactor with glass wool. Prior to each experiment, the catalyst was reduced overnight at 250°C in 10 sccm of flowing hydrogen.

The reactor was inserted into a modified Xytel CBX/5A catalyst activity unit, shown schematically in Fig. 1. Hydrogen or hydrogen/ammonia mixtures were presaturated with liquid substrates in a saturator fabricated from a 45-ml cup of a Paar 1991 ACK kinetic apparatus. Gas was sparged into the saturator through a Type 316 stainless-steel HPLC solvent frit. The substrate-saturated gas could be diluted further with additional hydrogen; all gas flow rates were controlled with mass flow controllers (Brooks Model 5810 mass flow sensor with Model 5835A control valve). Gases flowed to and from the reactor through heated Type 316 stainless-steel lines.

Reactant and product stream compositions were analyzed by on-line gas chroma-

tography (Perkin–Elmer Model 2000) using a 20 m × 0.25 mm DB-1 fused silica capillary column, increasing the column temperature from 45 to 250°C at 6°C/min. Samples were taken with a heated gas-sampling valve (Valco Model C10T) equipped with an 0.1-ml sample loop. The FID detector response to each component was measured independently. Products were identified according to their retention times, and their identification was corroborated by GC-MS analysis (Hewlett–Packard Series 5970 GC/EIMS).

An IBM PC-XT was used to monitor and control gas flow rates, gas handling system and reactor temperatures, and the gas chromatograph. Analog signals from the GC were digitized, integrated, and stored with a Nelson analytical Series 760 interface and Series 3000 chromatography data system.

All X-ray photoelectron spectra were measured with a Physical Electronics Model 55 X-ray photoelectron spectrometer equipped with a Mg$K\alpha$ anode source (1253.6 eV). The adventitious carbon 1S line at 285.0 eV was used for charge referencing. The energy scale of the spectrometer was calibrated using the Au $4F_{7/2}$ = 83.3 eV, Cu $2p_{3/2}$ = 932.4 eV, and Cu $3p_{2/3}$ = 74.9 eV photoelectron lines. The analyzer pass energy was 25 eV for high-resolution studies, while 100 eV was used for routine survey scans. All catalyst samples were studied as fine powders mounted on polymer film-based adhesive tape with a metallic backing.

A Joel 100 series transmission electron microscope was used in the TEM studies. Samples were prepared by ultramicrotomy. X-ray diffraction patterns were measured with a Siemens X-ray diffractometer.

III. RESULTS

1. Reaction Network

The primary goal of this work was to determine the HDN reaction network of quinoline and the regioselective reduction product, 1,2,3,4-tetrahydroquinoline. To accomplish this, we determined quantitatively the product distributions of the gas-phase reactions of quinoline and 1,2,3,4-tetrahydroquinoline and their major products at 250°C under 1 atm of hydrogen. The reactants (substrates) are listed in Fig. 2; they include quinoline, **1,** its partially reduced products 1,2,3,4-tetrahydroquinoline, **2,** and 5,6,7,8-tetrahydroquinoline, **3,** as well as 2-propylaniline, **4,** and propylbenzene, **5.** In all experiments, the substrate concentration was 2 mol%. Product distributions were measured as a function of the space time, τ, defined as the weight of catalyst in the reactor divided by the substrate molar flow rate.

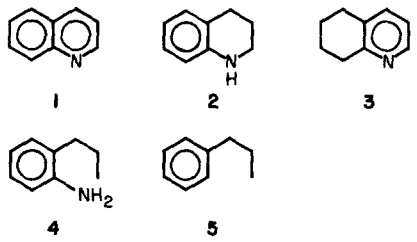

FIG. 2. HDN model compounds.

Well over 70 compounds were produced in the reactions of quinoline and its partially reduced isomers. The major products were alkylanilines, alkylbenzens, alkylcyclohexanes, and methane, with smaller amounts of indoles, indene, indane, and 2-methylquinoline. Carbon atom balances were computed in each experiment by assuming that all unidentified species contained eight carbon atoms each; carbon balance closures were better than 10% in all experiments.

On exposure to all substrates, catalyst activity decreased monotonically and became negligible after 24 hr on stream. Because of the low hydrogen pressures in this study, we believe that deactivation is caused by coke formation. This hypothesis is supported by the observation that catalyst activity could be regained by oxidizing the catalyst in air and subsequently reducing it in hydrogen. Catalyst deactivation complicated the interpretation of experi-

TABLE 1

Product Distributions in the HDN Reaction of 1,2,3,4-Tetrahydroquinoline, 2-Propylaniline, and Propylbenzene

Product	Substrate yield (%)		
	1,2,3,4-Tetrahydroquinoline[a]	2-Propylaniline[b]	Propylbenzene[c]
Methane[d]	2.8	2.9	2.4
Cyclohexane	0.6	1.2	2.5
Methylcyclohexane	0.0	0.6	6.9
Ethylcyclohexane	0.0	0.1	5.1
Propylcyclohexane	0.0	2.1	21.8
Benzene	4.4	10.7	3.1
Toluene	2.3	3.1	19.6
Ethylbenzene	0.4	1.0	6.1
Propylbenzene	0.6	17.7	0.0
Aniline	14.0	4.8	—
2-Methylaniline	23.5	5.1	—
2-Ethylaniline	16.0	2.1	—
2-Propylaniline	0.0	0.0	—
Quinoline	5.4	0.0	—
1,2,3,4-Tetrahydroquinoline	0.0	0.0	—
5,6,7,8-Tetrahydroquinoline	6.4	0.0	—
2-Methylindole	0.1	0.0	—
Indole	2.8	0.0	—
Indene	2.8	0.0	0.0
Indane	0.3	0.3	0.0
2-Methylquinoline	2.2	0.0	—
Other	15.4	14.8	15.4

[a] τ = 2182 g hr/mol.
[b] τ = 669 g hr/mol.
[c] τ = 820 g hr/mol.
[d] Methane produced by complete hydrogenolysis of substrate.

mental results, as it was necessary to measure product distributions and reaction rates at constant levels of catalyst activity. We found that the catalyst activity correlated well with an exposure parameter, ϕ, defined as the amount of substrate that passed through the reactor per gram of catalyst (*17*). In the discussion that follows, product distributions were measured as a function of space time at ϕ = 0.0013 mol substrate/g catalyst unless otherwise specified.

i. Quinoline and 1,2,3,4-tetrahydroquinoline. A typical product distribution from the HDN of **2** is listed in Table 1. The predominant products include **1, 3,** alkylanilines, and alkylbenzenes. Only a very small amount of cyclohexane was observed, and no decahydroquinoline was detected. The variation of this product distribution with space time is shown in Fig. 3a. For clarity, we have grouped structurally similar compounds in this and subsequent figures. In general, species in each group differ only by the length of their aliphatic side chain. An exception to this is the combining of compounds **1** and **3;** as is discussed below, these compounds interconvert rapidly, and

3 does not undergo further reduction. Also, indane and indene have been grouped with the alkylbenzenes.

The yield of **1** and **3** increases sharply at short space times and subsequently decreases. Since neither decahydroquinoline nor alkylpyridines was observed, this behavior indicates that **2** is rapidly dehydrogenated to **1**, and that reduction of **1** to both **2** and **3** is rapid and reversible. The alkylaniline concentration increases significantly at intermediate space times, presumably by hydrogenolysis of the alkyl C–N bond of **2**. The aniline yield becomes reasonably constant at large space times, probably reflecting slow reduction to subsequent products. The predominant HDN products are the alkylbenzenes, which appear in small amounts at longer space times.

HDN of **1** produces essentially the same product distribution as that of **2**. Comparison of Fig. 3a with 3b, which shows the variation of the product distribution in the HDN of **1** with τ, indicates that compounds **1** and **2** react with hydrogen in a nearly identical fashion. HDN of **3** is also quite similar, as shown by Fig. 3c. The strong similarity between the product yields of **1** and the tetrahydroquinoline isomers is further evidence of rapid and reversible hydrogenation of **1** to the two tetrahydroquinoline isomers. The absence of decahydroquinoline and alkylpyridines indicates that **3** undergoes no further reaction and also suggests that complete hydrogenation of **1** is not required for C–N bond hydrogenolysis in this system.

ii. 2-Propylaniline and propylbenzene. The fate of the first C–N bond cleavage products, the alkylanilines, was determined by examining the product distribution in the HDN of **4**. As shown in Fig. 4a, **4** is converted at short and moderate space times to alkylanilines with negligible production of alkylcyclohexanes. At longer space times, the yield of the cyclohexanes begins to increase at the expense of the alkylbenzenes. This is shown more clearly in Fig. 4b, which shows that alkylcyclohexanes are the primary product of the hydrogenation

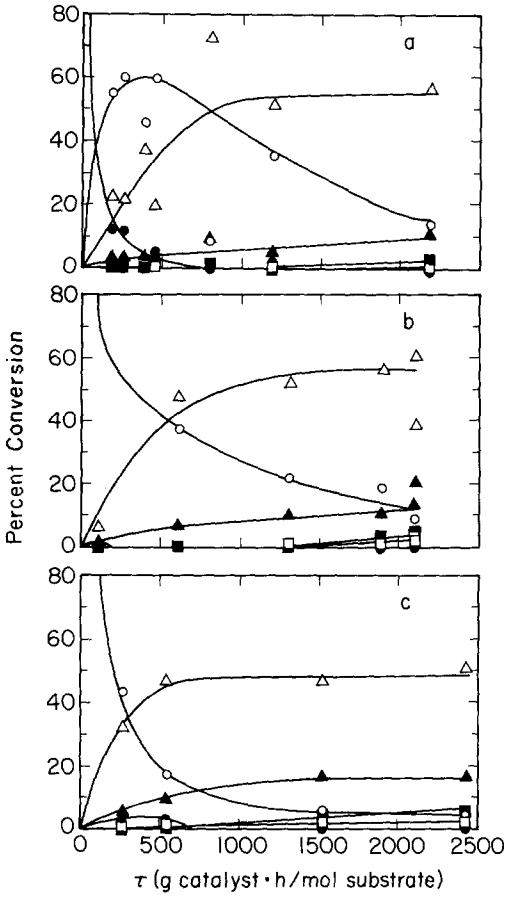

FIG. 3. HDN product distribution profiles: (a) 1,2,3,4-tetrahydroquinoline, (b) quinoline, (c) 5,6,7,8-tetrahydroquinoline. (●) 1,2,3,4-Tetrahydroquinoline, (○) quinoline + 5,6,7,8-tetrahydroquinoline, (△) alkylanilines, (▲) alkylbenzenes, (□) alkylcyclohexanes, (■) methane.

of **5** under the same conditions. This suggests that HDN of the alkylanilines precedes hydrogenation of the aromatic ring. Table 1 indicates that side-chain hydrogenolysis is significant in the reaction of both substrates. For example, HDN of **4** at τ = 669 g hr/mol produces alkylanilines comprised of 40% aniline, 43% 2-methylaniline, and 17% 2-ethylaniline. Indane is also observed, perhaps produced via a free radical intermediate of **4** following final C–N bond cleavage.

2. *Catalyst Poisoning*

The experimental results that we have presented have shown that the nickel/sil-

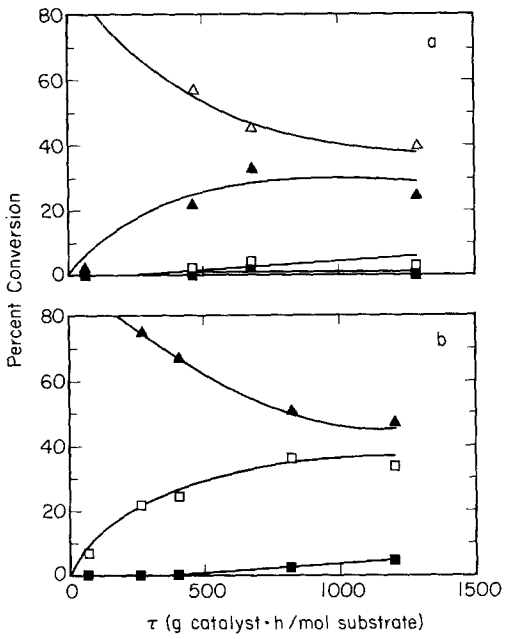

FIG. 4. HDN product distribution profiles: (a) 2-propylaniline, (b) propylbenzene. (△) Alkylanilines, (▲) alkybenzenes, (□) alkylcyclohexanes, (■) methane.

ica–alumina catalyst promotes two general reactions: hydrogenation and hydrogenolysis. A metal is typically required to promote hydrogenation, while hydrogenolysis is often accomplished with acidic catalysts, such as silica–alumina. However, it has been shown previously that acidic sites alone are not able to perform HDN chemistry. In one example, a zeolite was shown to be inactive to C–N bond cleavage HDN of **2** (*18*). Katzer and co-workers (*19*) showed that both acidic and metal sites are required to cleave C–N bonds. In this two-site mechanism, the acidic site acts as an electrophile and promotes bond-breaking activity. The metal site acts as an electron-donating site and coordinates the transfer of hydrogen associated with bond dissociation. This mechanism is similar to a Hoffman E-2 type elimination (*20, 21*).

To test whether this model accurately describes this catalyst, a series of selective poisoning studies was conducted. In the first, the catalyst was presulfided to eliminate the activity of the metal (*22*); this should affect both hydrogenation and hydrogenolysis. In the second, ammonia was added to the feed mixture in an effort to neutralize the acidic sites; this should affect hydrogenolysis alone, if the acidic sites are required for C–N bond scission.

The 50% nickel/silica–alumina catalyst was presulfided with 15% H_2S (balance hydrogen) for 8 hr at 300°C. The poisoned catalyst showed no activity for HDN of **2** at 250°C and 1 atm of hydrogen. Since hydrogen sulfide poisons both nickel and nickel oxide (*23*), this result implies that nickel sites are required for HDN, in agreement with Katzer's model (*19*).

Two experiments involving addition of ammonia to the reactor feed were performed. In the first experiment, 30 mol% NH_3 was added to a mixture of 2 mol% **2** in hydrogen. There was no consistent change in the product distribution or reaction kinetics, suggesting that the acidic sites on the catalyst support make little contribution to the reaction network. Alternately, these sites could be immediately neutralized by **2** and other bases produced during HDN. In the second experiment, 2 mol% of NH_3 was added to a mixture of 2 mol% **5** in hydrogen. This concentration of ammonia was chosen to approximate the basicity of the reactants during HDN of **1.** At low conversion (small space time), the ammonia had no effect on the reaction kinetics or product distribution. At longer space times, however, a notable increase in the amount of hydrogenated products was observed. This observation is in contrast to the results of Satterfield and co-workers (*24*) who observed an eightfold decrease in the hydrogenation rate of **5** over a commercial HDN catalyst. Our result is unexpected and a satisfactory explanation has not been determined.

3. Catalyst Characterization

The morphology and composition of the catalyst were characterized by X-ray photoelectron spectroscopy (XPS), transmission electron microscopy (TEM), and X-ray diffraction (XRD). New and used

samples of both the untreated and presulfided catalyst were examined using XPS. Only the untreated catalyst was studied with TEM and XRD.

XPS spectra of both the new and used catalyst showed the expected silicon and nickel photoemission lines, along with those of aluminum. The nickel $2p_{3/2}$ binding energy for both the used and the new catalyst were essentially identical at 856.5 and 856.6 eV, respectively. In contrast, the "shake-up" satellite positions (*25*) were different (862.7 and 861.7 eV, respectively), indicating some difference between the surfaces.

The nickel $2p_{3/2}$ binding energies were a full 2.5 eV higher than the 854.0 eV binding energy observed for the high-purity NiO (99.99%) standard used in this study and the values reported by other workers (*26–28*). In addition, the line shapes of the Ni $2p_{3/2}$ lines were different from those reported for NiO. Rather, the binding energy data were more consistent with a ternary nickel oxide or a higher valent nickel system. Indeed, binding energy and satellite data for the catalyst samples were very close to those reported for $NiAl_2O_4$ and Ni_2O_3 (*29*). These XPS studies clearly show that nickel is present in a 2+ or higher oxidation state on the surface of the supported nickel crystallites. They also suggest that nickel may react with the alumina in the support to form an aluminate.

An XPS study of new and used samples of the presulfided catalyst was also conducted. Again, we observed the expected silicon, nickel, and sulfur photoemission lines, along with those of aluminum. The nickel $2p$ binding energy showed a shift of 0.9 eV between the used and new samples (857.4 and 856.5 eV, respectively). The explanation of this shift is not apparent, but it may be due to sample charging. Clearly, the nickel $2p$ binding energies indicate a nickel 2+ or higher valence. The sulfur $2p_{3/2,1/2}$ lines of the new and used presulfided catalyst samples were observed at 163.0 and 162.8 eV, respectively; these are consistent with a metal sulfide species (*30*). There is also evidence for sulfates and elemental sulfur on the surface. These are presumably due to oxidation of the catalyst sample during transfer from the pretreatment apparatus to the XPS spectrometer.

Transmission electron micrographs of new and used catalyst samples are shown in Figs. 5a and 5b, respectively. These micrographs show a homogeneous distribution of metal particles on the order of 80 to 100 Å in size. The used sample had slightly larger particles, indicating that some sintering occurred during reaction. The electron diffraction patterns for both the new and used catalysts were identical and showed that the metal crystallites were a mixture of nickel phases.

The XRD pattern of the unused catalyst contained strong but broad Ni-metal peaks. The pattern also contained broad peaks of a second phase consistent with nickel aluminate. The nickel metal crystallite size was approximately 50 Å. Comparison to the TEM and XPS measurements suggests that the individual supported metal particles consisted of a nickel metal core covered by several atomic layers of nickel oxide and/or aluminate. The nickel peaks in the XRD pattern of the used catalyst were stronger and sharper. This implies that some of the surface Ni 2+ was converted to nickel metal with a concomitant increase in average crystallite size during reaction.

IV. DISCUSSION

1. HDN Reaction Network

The kinetic measurements indicate that HDN of **1, 2** and **3** occurs via the reaction pathway shown in Fig. 6. As shown, substrate **2** is rapidly dehydrogenated to **1.** This is rapidly and reversibly hydrogenated to **3,** which undergoes no other reactions. Thus, substrate **3** is not converted to decahydroquinoline in the reaction network, and all of this substrate ultimately reacts through the same pathway as that of substrate **2.** The primary HDN network involves C–N bond

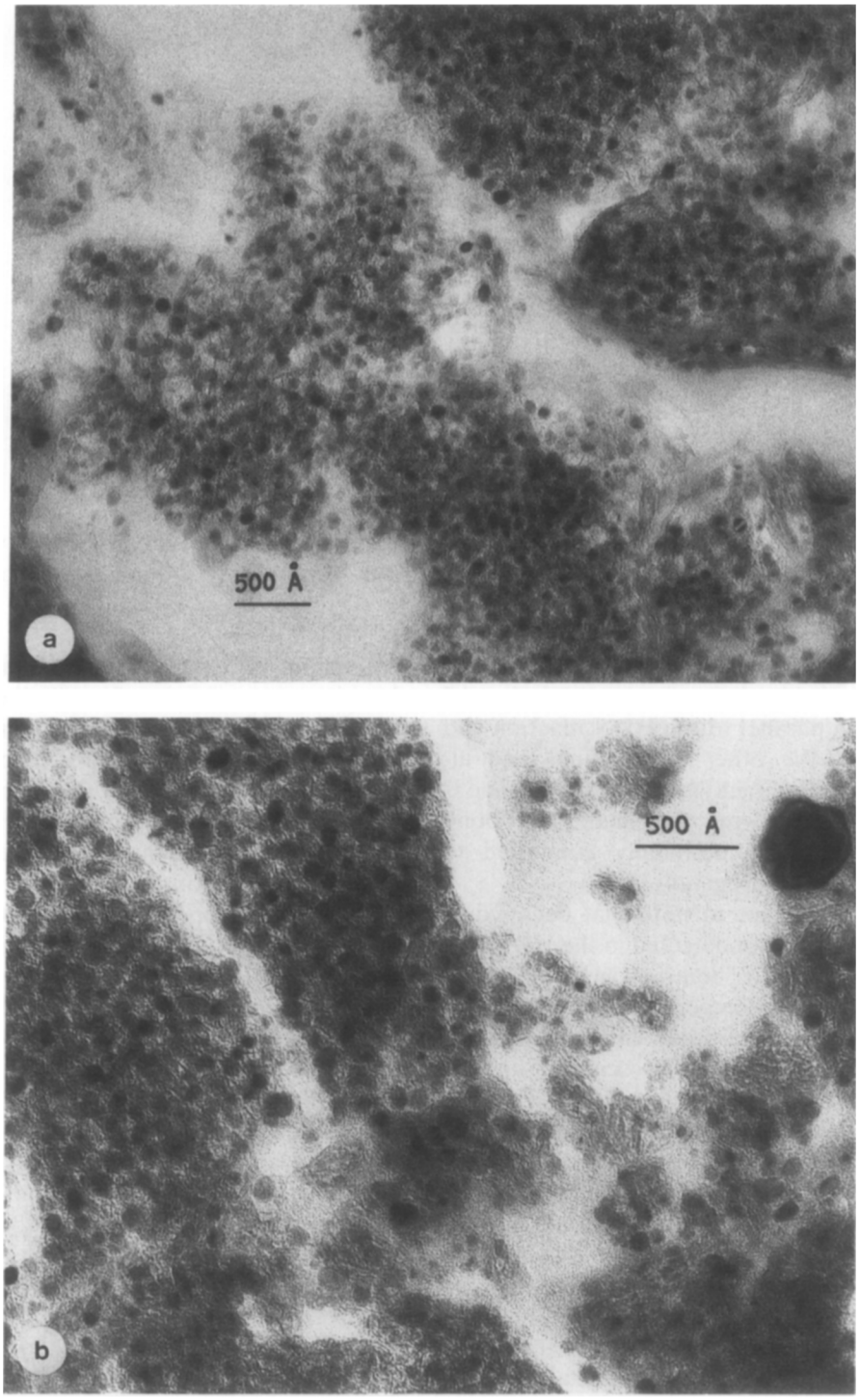

FIG. 5. Transmission electron micrographs of catalyst: (a) new sample, (b) used sample.

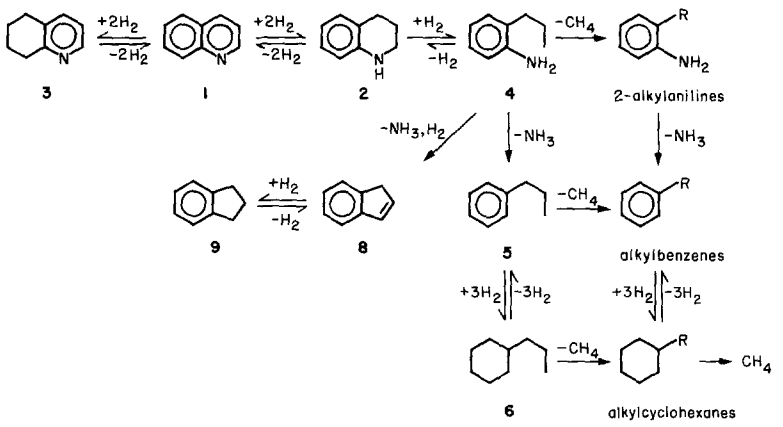

FIG. 6. HDN reaction network of 1,2,3,4-tetrahydroquinoline.

scission of substrate **2** to form **4** and subsequent loss of ammonia to form **5.** We speculate that **4** is also the precursor to ring-closure products indene and indane via a free-radical mechanism. Hydrogenolysis of the propyl side chain of compounds **4** and **5** occurs in parallel to the HDN reaction and produces the other alkylanilines and alkylbenzenes. Finally, propylcyclohexane is produced following the final C–N bond scission; this is ultimately converted to methane by hydrogenolysis.

It is important to note that decahydroquinoline was not detected in the HDN of **2** and **3;** this is in contrast to liquid-phase HDN at higher temperature and pressures, in which decahydroquinoline is a primary precursor to C–N bond scission in substrate **1** (*1–6*). Equally significant is the observation of ammonia removal from **4** prior to hydrogenation of the aromatic ring. This, also, is in contrast to HDN under more severe conditions (*1–7*), in which alkylcyclohexylamines are formed prior to ammonia loss. These results also indicate that the presence of the anilines may have a profound effect on the selectivity of the highly loaded nickel/silica–alumina catalyst by reducing the hydrogenation rate of the alkylbenzenes. This is illustrated in the reactions of **4** and **5** at long space times: **4** yielded only 5% cyclohexyl derivatives, while **5** yielded 36% alkylcyclohexanes.

2. HDN Kinetics

While the 50% nickel/silica–alumina catalyst is more selective for alkylbenzenes than existing HDN catalysts, its activity for HDN must be comparable for it to be potentially useful. In an effort to determine its activity, we determined pseudo-first-order rate constants for the major HDN reactions of **1.** These rate constants allow an order-of-magnitude comparison of the activity of this catalyst to commercial HDN catalysts.

A simplified reaction network was chosen to model the HDN network of **2;** this is shown in Table 2. The actual network was simplified by ignoring dealkylation reactions and combining components **1** and **3** into a single pseudocomponent. Since our primary goal was to estimate C–N bond cleavage rate constants, we did not believe that important information would be lost by determining group reaction rates. All reactions were assumed to be first-order in hydrocarbon and zero-order in hydrogen.

Rate constants for the six reactions were determined by the method of Himmelblau *et al.* (*31*) with a weighting factor of unity. The kinetic model was fit to the reaction data of **2;** the best-fit rate constants are

TABLE 2

Pseudo-First-Order Rate Constants of Quinoline HDN over 50% Ni/SiO_2–Al_2O_3 at 250°C and 1 atm Hydrogen

Simplified reaction network
$A \underset{k_2}{\overset{k_1}{\rightleftarrows}} B \xrightarrow{k_3} C \xrightarrow{k_4} D \xrightarrow{k_5} E \xrightarrow{k_6} F$
A = 1 + 3
B = 2
C = 2-alkylanilines
D = alkylbenzenes
E = alkylcyclohexanes
F = methane
Pseudo-first-order rate constants
$k_1 = 2.0 \times 10^{-3}$ mol/hr g
$k_2 = 1.0 \times 10^{-2}$
$k_3 = 4.5 \times 10^{-3}$
$k_4 = 2 \times 10^{-4}$
$k_5 = 2 \times 10^{-4}$
$k_6 = 1 \times 10^{-2}$

listed in Table 2, and calculated product distribution is shown in Fig. 7. The model underestimates the reactivity of **2** after τ = 250 g hr/mol, and the maximum in the yield of compounds **1** and **3** occurs at too short a space time. The calculated alkylaniline yield is overestimated at short space times. Fair agreement is seen for alkylbenzene, alkylcyclohexane, and methane production. The yield profiles were quite sensitive to rate constants k_1 through k_3 and less sensitive to the remaining constants. While the agreement between model and data is by no means quantitative, the model should be satisfactory for an order-of-magnitude estimate of catalytic activity.

Cocchetto and Satterfied (*3*) report pseudo-first-order rate constants for nitrogen removal from alkylanilines and decahydroquinoline during HDN of **1** over a commercial HDN catalyst at 330°C and 7.0 mPa of hydrogen; the rate constants were 2×10^{-3} g hr/mol and 2×10^{-4} g hr/mol, respectively. The comparable rate constant in this study is the alkylaniline denitrogenation rate constant, $k_4 = 2 \times 10^{-4}$ g hr/mol. Since decahydroquinoline is the predominant HDN intermediate over the commercial catalyst, this suggests that the activity of the 50% Ni/silica–alumina catalyst is of the same order of magnitude as that of the commercial catalyst. It is noteworthy that this study was performed at a temperature 80°C lower than that of commercial HDN processes, suggesting that the highly loaded nickel catalyst may actually be more active on a weight basis than the commercial catalyst. We cannot, however, exclude the possibility that a commercial catalyst operating under the same mild conditions might show similar selectivity and activity.

3. Possible Bonding Modes of Quinoline to Nickel

We speculate that differences in the modes of bonding of **1** and **2** to the supported Ni^{2+} ions may contribute to the observations discussed above. The availability of nonbonding electrons on the nitrogen atom may be a significant parameter in the bonding of mono- and polynuclear heteroaromatic nitrogen compounds to supported metal centers. For example, a recent study using pyridine in H–D exchange re-

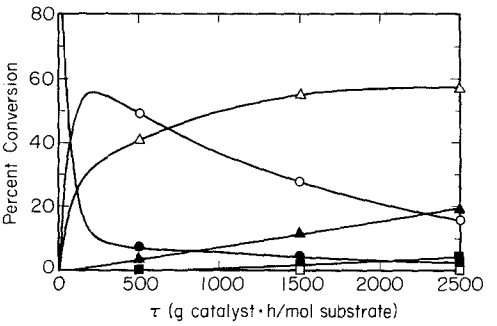

FIG. 7. Calculated product distribution profile of 1,2,3,4-tetrahydroquinoline. (●) 1,2,3,4-Tetrahydroquinoline, (○) quinoline + 5,6,7,8-tetrahydroquinoline, (△) alkylanilines, (▲) alkylbenzenes, (□) alkylcyclohexanes, (■) methane.

actions on a nickel (100) surface strongly suggested α-pyridyl or bridging α-pyridyl complexes as intermediates (*32*). We envision a similar bonding mode (μ_2–η^2) for substrate **1,** shown in Fig. 8, that also has precedent in model compound studies with a Ru trinuclear cluster, $Ru_3(CO)_{12}$ (*33*). Also, with $Ru_3(CO)_{12}$, substrate **2** underwent a dehydrogenation reaction to form **1** and 3,4-dihydroquinoline; both bonded μ_2–η^2 to the ruthenium triangle. In addition, recent studies from our laboratory also provided unequivocal evidence that **2** bonds to a mononuclear rhodium center, (pentamethylcyclopentadienyl)rhodium cation (Cp^*Rh^{2+}) via the π system of the benzene ring (η^6), while **1** bonds through the nitrogen nonbonding electrons (η^1, N) (*15*).

It is conceivable then that the η^6 and the μ_2–η^2 bonding modes for **2** to the supported Ni^{2+} ions may provide important intermediates for the cleavage of the C–N bond to give **4** as well as dehydrogenation to give **1;** these bonding modes are shown in Fig. 8. The η^1, N bonding mode of **1** could be responsible for the regioselective hydrogenation of the nitrogen ring to provide **2** as was recently shown for the $Cp^*Rh(\eta^1$, N-quinoline$)^{2+}$ complex in selective hydrogenation experiments (*15*). Thus, hydrogenation–dehydrogenation and carbon–nitrogen cleavage reactions are possibly controlled by the various bonding modes of the substrates to the supported Ni^{2+} ions.

Finally, the fact that **3** is the only significant aromatic ring hydrogenated product detected in our HDN network may be attributed to an η^6 bonding mode of substrate **1** via an intramolecular rearrangement of the η^1, N bonding mode (N to π), followed by hydrogenation–dehydrogenation (**1**⇆**3**). We have recently discovered this type of intramolecular N to π rearrangement with a (cyclopentadienyl)ruthenium(η^1, N–quinoline)$^+$ complex (*34*). Thus, we feel that these various bonding modes of **1** and **2** with homogeneous examples may have some relevance to heterogeneous catalysis.

μ_2-η^2 - Quinolinedinickel Complex

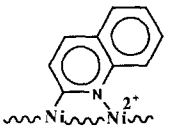

η^1 - N-Quinolinenickel Complex

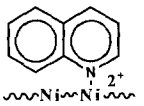

η^6 - Quinolinenickel Complex

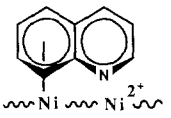

η^6 - 1,2,3,4-Tetrahydroquinolinenickel Complex

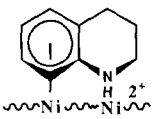

μ_2 - η^2 - 1,2,3,4-Tetrahydroquinolinedinickel Complex

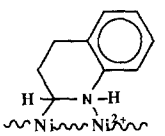

FIG. 8. Possible bonding modes of quinoline and 1,2,3,4-tetrahydroquinoline to Ni^{2+} supported on silica–alumina.

V. CONCLUSIONS

The activity and selectivity of a 50% nickel oxide/aluminate on silica–alumina catalyst for hydrodenitrogenation of compounds **1** and **2** has been investigated. At 250°C and under 1 atm of hydrogen, the carbon–nitrogen bonds in 1,2,3,4-tetrahydroquinoline and the formed alkylanilines are cleaved without hydrogenation of the aromatic ring. This is in contrast to commercial HDN processes in which alkylcyclohexanes are produced subsequent to nitrogen removal as ammonia. The catalyst is active for side-chain hydrogenolysis, but relatively inactive for complete hydrogenolysis of the aromatic rings. Despite an 80°C difference in operating temperature,

the activity of this catalyst is within an order of magnitude of that of a commercial HDN catalyst, which operate at higher temperatures and pressures.

Catalyst deactivation, presumably by coking, is observed. Complete reactivation of the catalyst is possible by oxidation in air and subsequent reduction in hydrogen. The catalyst is quickly and irreversible poisoned by sulfur. Ammonia appears to increase the hydrogenation activity of the catalyst, suggesting that acidic sites have a limited role in the activity of the catalyst. Characterization of the catalyst by XPS, XRD, and TEM indicates that a Ni^{2+} or higher valent species, possibly $NiAlO_4$, may be the active catalyst for HDN. Finally, the C–N cleavage and selective hydrogenation reactions are thought to occur by specific bonding modes of the substrates to the Ni^{2+} binding sites.

ACKNOWLEDGMENTS

This study was supported by the Assistant Secretary of Fossil Energy, Office of Technical Coordination, U.S. Department of Energy through the Pittsburgh Energy Technology Center, Pittsburgh, Pennsylvania, under Contract DE-ACO3-76SF00098. We give special thanks to Dr. I. Y. Chan and Dr. R. C. Medrud of Chevron Research Co. for providing the TEM, XRD, and electron diffraction measurements. We also thank Dr. D. L. Perry of Lawrence Berkeley Laboratory for measurement and interpretation of XPS spectra and Karl Russ of United Catalysts, Inc., for a generous sample of the catalyst used in this study.

REFERENCES

1. Sonemans, J., Van den Berg, G. H., and Mars, P., *J. Catal.* **31,** 220 (1973).
2. Satterfield, C. N., Modell, M., and Wilkers, J. A., *Ind. Eng. Chem. Proc. Des. Dev.* **20,** 62 (1981).
3. Cocchetto, J. F., and Satterfield, C. N., *Ind. Eng. Chem. Proc. Des. Dev.* **20,** 49 (1981).
4. Satterfield, C. N., and Yang, S. H., *Ind. Eng. Chem. Proc. Des. Dev.* **23,** 11 (1984).
5. Stern, E. W., *J. Catal.* **57,** 390 (1979).
6. Bhinde, M. V., Shih, S., Sawadski, R., Katzer, J. R., and Kwart, H., "Chemistry and Uses of Molybdenum," 3rd Int. Conf., 184 (1979).
7. Laine, R. M., *Catal. Rev. Sci. Eng.* **25,** 459 (1983).
8. Moreau, C., Durand, R., Zimimita, N., and Geneste, P., *J. Catal.* **112,** 411 (1988).
9. Schulz, H., Schon, M., and Rahman, N. M., *in* "Studies in Surface Science and Catalysis" (L. Cerveny, Ed.) Vol. 27, Chap. 6, p. 201. Elsevier, Amsterdam, 1986.
10. Fish, R. H., Thormodsen, A. D., and Cremer, G. A., *J. Amer. Chem. Soc.* **104,** 5234 (1982).
11. Fish, R. H., Tan, J. L., and Thormodsen, A. D., *J. Org. Chem.* **49,** 4500 (1984).
12. Fish, R. H., *Ann. N.Y. Acad. Sci.* **415,** 292 (1983).
13. Fish, R. H., Thormodsen, A. D., and Heinemann, H., *J. Mol. Catal.* **31,** 191 (1985).
14. Fish, R. H., Tan, J. L., and Thormodsen, A. D., *Organometallics* **4,** 1743 (1985).
15. Fish, R. H., Kim, H.-S., Babin, J. E., and Adams, R. D., *Organometallics* **7,** 2250 (1988).
16. Fish, R. H., Thormodsen, A. D., Moore, R. S., Perry, D. L., and Heinemann, H., *J. Catal.* **102,** 270 (1986).
17. Moore, R. S., M.S. thesis, University of California at Berkeley, 1988.
18. Thormodsen, A. D., Ph.D. thesis, University of California at Berkeley, 1985.
19. Katzer, J. R., Stiles, A. B., and Kwart, H., "Development of Unique Catalysts for Hydrodenitrogenation of Coal-Derived Liquids," DOE/ET/03297-1, 1980.
20. Nelson, N., and Levy, R. B., *J. Catal.* **58,** 489 (1979).
21. Olalde, A., and Perot, G., *Appl. Catal.* **13,** 373 (1985).
22. Satterfield, C. N., and Gultikin, S., *Ind. Eng. Chem. Proc. Des. Dev.* **20,** 62 (1981).
23. Butt, J. B., Joyal, C. W. M., and Megris, C. E., *in* "Catalyst Deactivation" (E. E. Petersen and A. T. Bell, Eds.), Dekker, New York, 1987.
24. Gultikin, S., Ali, S. A., and Satterfield, C. N., *Ind. Eng. Chem. Proc. Des. Dev.* **23,** 181 (1984).
25. Veron, G. A., Stuckey, G., and Carlson, T. A., *Inorg. Chem.* **15,** 278 (1976).
26. Matienzo, L. J., Yin, L. O., Grim, S. O., and Swatz, W. E., *Inorg. Chem.* **12,** 2762 (1973).
27. Dufresne, P., Payen, E., Grimblot, J., and Bonnelle, J. P., *J. Phys. Chem.* **85,** 2344 (1981).
28. Narayanan, S., and Uma, K., *J. Chem. Soc. Faraday Trans. 1* **81,** 2733 (1985).
29. Ng, K. T., and Hercules, D. M., *J. Phys. Chem.* **80,** 2095 (1976).
30. Lindberg, B. J., Hamrin, K., Johansson, G., Gelius, U., Fahlman, A., Nordling, C., and Siegbahn, K., *Phys. Scr.* **1,** 286 (1970).
31. Himmelblau, D. M., Jones, C. R., and Bischoff, K. B., *Ind. Eng. Chem. Fund.* **6,** 539 (1967).
32. Wexler, R. M., Tsai, M., Friend, C. M., and Muetterties, E. L., *J. Amer. Chem. Soc.* **104,** 2034 (1982).
33. Fish, R. H., Kim, T.-J., Stewart, J. L., Bushweller, J. H., Rosen, R. K., and Dupon, J. W., *Organometallics* **5,** 2193 (1986).
34. Fish, R. H., Kim, H.-S., and Fong, R. H., *Organometallics* **8,** 1375 (1989).